Journal of Organometallic Chemistry, 372 (1989) 25–32
Elsevier Sequoia S.A., Lausanne – Printed in The Netherlands
JOM 09821

Tin–iron carbonyl clusters from the reaction of stannane, SnH_4, with $Fe_2(CO)_9$; the crystal structure of $SnFe_5(CO)_{19}$ *

Skelte G. Anema, Kenneth M. Mackay and Brian K. Nicholson
School of Science, University of Waikato, Hamilton (New Zealand)

(Received October 24th, 1988)

Abstract

SnH_4 reacts with $Fe_2(CO)_9$ under restricted conditions to form the known compound $Sn[Fe_2(CO)_8]_2$ (**1**), and a new tin-iron cluster $SnFe_5(CO)_{19}$ (**2**). The crystal structure of **2** shows a structure with an Fe_3 triangle edge-bridged by a $SnFe_2$ one. Further tin-iron clusters are indicated.

Introduction

A classic cluster molecule, $Sn[Fe_2(CO)_8]_2$ (**1a**), was reported twenty-one years ago in a seminal study on tin-iron carbonyl compounds [1,2]. More recently, Ge (**1b**) [3,4], Pb (**1c**) [5], and Si (**1d**) [6] analogues have been structurally characterised.

Since the reactions of GeH_4 [7], or SiH_4 [8], with $Co_2(CO)_8$ under mild conditions proved to be a useful route to $E[Co_2(CO)_7]_2$ (E = Ge (**2a**) [7], E = Si (**2b**) [8]) clusters, isoelectronic with **1**, the analogous reactions of the hydrides with $Fe_2(CO)_9$ were investigated. For E = Si, a good yield of **1d** was obtained from SiH_4 [6], while improved but variable yields of **1b** were obtained from GeH_4 [6]. The variability in the germanium reactions was traced to the formation of two further compounds, $Ge_2Fe_6(CO)_{23}$ and $Ge_2Fe_7(CO)_{26}$ [9].

The success of these hydride experiments led us to examine the reaction of stannane with $Fe_2(CO)_9$ under similar conditions, despite the relatively low stability [10] of SnH_4.

Results and discussion

In the reaction of SnH_4 with $Fe_2(CO)_9$ in hexane, there is a fairly narrow window of conditions which avoid predominance of the stannane decomposition.

---

* Dedicated to Professor H.J. Emeléus in his 85th year. K.M.M., who was introduced to Group 14 hydrides at Cambridge, hopes Professor Emeléus will find this synthetic application of stannane (compare [10]) an appropriate tribute.

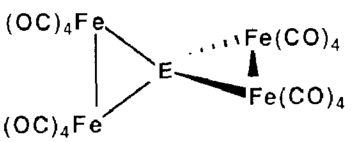

1a. E = Sn
1b. E = Ge
1c. E = Pb
1d. E = Si

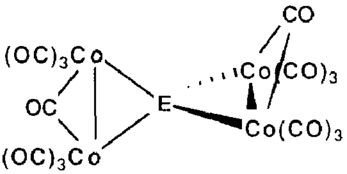

2a. E = Ge
2b. E = Si

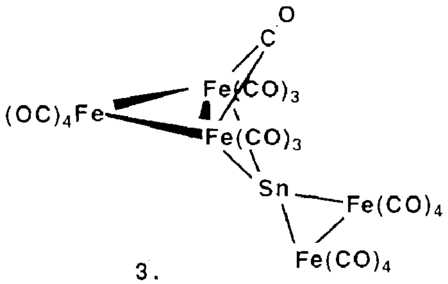

3.

Below 35 °C or above 70 °C, production of Sn metal and $Fe_3(CO)_{12}$ from SnH_4 and $Fe_2(CO)_9$ was the dominant process. Fortunately, a brief reaction time at 68 °C does allow formation of tin-iron clusters and about 40% of the tin was found in the isolated products. The balance was undoubtedly lost during workup, as the fractions decomposed slowly during chromatography. At 68 °C, the initial colour change was to orange then red, not to the green of $Fe_3(CO)_{12}$ as observed under the other conditions tried. The hydrogen from the SnH_4 was quantitatively recovered as H_2, together with a little CO, and both $Fe(CO)_5$ and $Fe_3(CO)_{12}$ were found. A TLC study showed four major mobile components in the product mixture following the $Fe_3(CO)_{12}$ band, together with three trace compounds and an immobile red-brown species. Separation by chromatography on silica gave the products listed in Table 1.

The first fraction had spectroscopic properties matching those reported [1] for **1a**. The early preparation [1] involved reaction of $Fe(CO)_5$ with Bu_3SnCl under forcing conditions. The present reaction is presumably comparable, proceeding via breaking

Table 1

Principal products from the reaction of SnH_4 with $Fe_2(CO)_9$.

Fraction	Colour	R_f [a]	Yield (%)	Comment
1	yellow	0.80	21	**1a**, properties as in ref. 1 and 6
2	brown	0.68	ca. 5	probable analogue of $Ge_2Fe_7(CO)_{26}$ [9]
3	orange	0.64	5–10	probable analogue of $Ge_2Fe_6(CO)_{23}$ [9]
4	green	0.47	19	new product (**3**)

[a] In 1/2 mixture of CH_2Cl_2/pentane: R_f of $Fe_3(CO)_{12}$ = 0.86.

of Sn–H bonds in place of Sn–C bonds, and under somewhat milder conditions reflecting the relative bond strengths. Since both the alkyl and the hydride substrates give a mixture of products, they are less convenient for the synthesis of **1a** than the halide coupling reactions [6].

The CO stretches have been measured in detail, with the solid state vibrations and the Raman activity reported for the first time. The Raman intensities tend to complement those in the infrared and a total of seven fundamentals are seen in solution. In the solid state spectra, a total of eleven frequencies were seen, of which seven coincided between Raman and infrared. While these absorptions in the solid may not all be fundamentals, these observations match very well with the prediction, for idealised D_{2d} molecular symmetry, that there are 11 Raman-active CO stretching modes and 7 infrared-active ones, all with Raman counterparts. Thus earlier tentative suggestions [1,3,4] that these compounds show vibrations of isolated *cis*-$Fe(CO)_4$ units must be abandoned.

Fractions 2 and 3 had very similar retention times and were only partially separable. Mixtures were obtained with different proportions of each component and these showed $\nu(CO)$ bands which allowed tentative identification as the tin species $Sn_2Fe_6(CO)_{23}$ and $Sn_2Fe_7(CO)_{26}$ (also in accord with the relative TLC mobilities) by comparison with the corresponding germanium species [9].

The fourth, green, fraction was identified as $SnFe_5(CO)_{19}$ (**3**) by the crystal structure determination, with spectroscopic properties in accord. The structure of $SnFe_5(CO)_{19}$ is illustrated in the figure and consists of an $SnFe_2$ triangle linked to an Fe_3 one via the spiro-tin atom. It can be regarded as a derivative of $Fe_3(CO)_{12}$ [11], with one of the bridging carbonyl ligands replaced by a $Sn[Fe_2(CO)_8]$ group. There is no disorder of the Fe_3 triangle of the type observed in $Fe_3(CO)_{12}$ and other M_3 clusters [11,12], no doubt because the commonly observed disorder requires a 60° rotation of the Fe_3 triangle which, for $SnFe_5(CO)_{19}$, would place the Sn atom in a terminal position as a stannylene ligand. Clearly a bridging SnR_2 group is more favoured. Alternatively, the structure of **3** may be related to that of $Sn[Fe_2(CO)_8]_2$ (**1a**) [2], with an extra $Fe(CO)_4$ group bridging one of the Fe–Fe bonds.

For the iron Group carbonyls there are three reasonable structures for 48-electron closed M_3 triangles: (i) an isosceles triangle with two bridging groups across the same edge, as in $Fe_3(CO)_{12}$, (ii) the unbridged equilateral triangle as in $Ru_3(CO)_{12}$, or (iii) the related equilateral triangle with single bridging groups across each side. For iron the first arrangement persists for a wide range of derivatives with different groups replacing a bridging ligand, e.g. $[Fe_3(CO)_{11}(\mu\text{-}H)]^-$ [13], $Fe_3(CO)_{11}(\mu\text{-}CNCF_3)$ [14], and is adopted for **3** despite the bulk of the bridging group μ-$Sn[Fe_2(CO)_8]$. This same arrangement is also adopted by the directly comparable ruthenium cluster $HBiRu_5(CO)_{18}$ which has μ-$Bi[Ru_2(CO)_8]$ and μ-H across one edge of the Ru_3 triangle [15]. However with two or more ER_2 substituents (E = Si, Ge, Sn) structures of type (iii) are found although this arrangement is not known among the parent binary carbonyls. Examples of this type are $Ru_3(CO)_9(\mu\text{-}GeMe_2)_3$ [16] and $Os_3(CO)_{10}(\mu\text{-}Sn\{CH(SiMe_3)_2\})_2$ [17].

An examination of the bond parameters for **3** shows that the unbridged sides of the Fe_3 triangle at 2.708 Å are slightly lengthened from those of $Fe_3(CO)_{12}$ (2.679 Å) while the bridged side is markedly increased from 2.588 to 2.658 Å. The Sn–Fe bonds to the Fe_3 triangle are longer at 2.588 Å than those to the $Fe_2(CO)_8$ group, average 2.55 Å, which is the reverse of the pattern found for the Bi–Ru bonds in the related $HBiRu_5(CO)_{18}$ [15]. The Fe–Fe bond of the $Fe_2(CO)_8$ group is longer at 2.878 Å than the other Fe–Fe bonds in the molecule, but compares closely with the corresponding bonds in $Sn[Fe_2(CO)_8]_2$, which are 2.87 Å [2].

The dihedral angle between the two $SnFe_2$ triangles sharing the spiro-Sn is exactly 90°, while the "butterfly" angle between the Fe_3 and $SnFe_2$ triangles is 123°. The angle between the Fe_3 triangle and the $Fe_2C(B)$ plane is only 105° which indicates that a rotation of the bridging groups about the Fe(2)–Fe(3) bond has taken place to reduce non-bonded interactions between the carbonyl groups on Fe(5) and those on the $Fe_3(CO)_{11}$ part of the molecule. Even with this widening, the shortest O...O non-bonded intramolecular distances are O(51)...O(12) 2.97 Å, O(53)...O(12) 3.10 Å and O(52)...O(23) 3.14 Å.

The formation of **3** in the reaction of SnH_4 with $Fe_2(CO)_9$ can be envisaged to take place via two alternative routes, both based on the generally observed ability of EH_2 (E = Si, Ge, Sn) groups to replace bridging CO ligands [18]. In the first alternative, initial formation of **1a** takes place with successive additions of the Sn centre across the Fe–Fe bonds of two molecules of $Fe_2(CO)_9$. Subsequent addition of a $Fe(CO)_4$ fragment (readily derived from $Fe_2(CO)_9$) to the Fe–Fe bond of one of the $SnFe_2$ triangles would generate **3**. The alternative route involves the initial formation of $Fe_2(CO)_8(\mu\text{-}SnH_2)$ which then displaces one of the bridging CO ligands from a molecule of $Fe_3(CO)_{12}$ which is also produced from $Fe_2(CO)_9$ under the reaction conditions.

This new structure, the presence of the two tentatively identified fractions, together with the indications of further minor or trace components, suggest that there is a rich chemistry of tin-iron clusters still to be explored. One intriguing possibility is $Sn[Fe_3(CO)_{11}]_2$, which would complete a series with **1a** and **3**, and would be formed by a repeat step in the first mechanism. There seems to be no steric constraint preventing the addition of an extra $Fe(CO)_4$ unit to **3**.

Experimental

SnH_4 was prepared and handled by literature methods [10]. Reactions were carried out in dry hexane in sealed tubes prepared under vacuum. Chromatography was performed on a Chromatotron (Harrison Research) with silica gel, or on standard silica preparative plates. Crystals were analysed for their metal ratio using electron probe analysis, with an ORTEC Energy-dispersive X-ray Analyser attached to a JEOL JS-M35 scanning electron microscope.

Reaction of SnH_4 with $Fe_2(CO)_9$.

At 68°C, $Fe_2(CO)_9$ (1.0 g, 2.75 mmol) and SnH_4 (0.44 mmol), were allowed to react in hexane (20 ml) with occasional shaking. Reaction occurred rapidly with bubbling and the clear solution became yellow, then brown, which darkened and the reaction was stopped when only a small amount of insoluble $Fe_2(CO)_9$ remained (about 20 min). Incondensable gases were recovered (1.18 mmol; 90% H_2, 10% CO) while the volatile fraction contained a significant amount of $Fe(CO)_5$ in the hexane (not separated) but no SnH_4. The involatile fraction was extracted from unreacted $Fe_2(CO)_9$ with CH_2Cl_2, and a TLC showed $Fe_3(CO)_{12}$ and four other major fractions (Table 1), together with three very minor mobile components (red R_f 0.71 and yellow, R_f 0.67 running very close to fractions 2 and 3; brown, running just ahead of fraction 4) and a red-brown, immobile species. Using radial chromatography on silica (Chromatotron), the bulk of the product was separated by eluting first with hexane to yield $Fe_3(CO)_{12}$ (not measured) and $Sn[Fe_2(CO)_8]_2$ (**1a**) (73 mg, 21%). Hexane/CH_2Cl_2 (1/1) removed the brown and orange fractions (2 and 3) together, but with considerable loss due to decomposition. Finally, CH_2Cl_2 eluted the slow-moving green fraction shown below to be $SnFe_5(CO)_{19}$ (**3**) (78 mg, 19%), again with some loss due to decomposition.

A similar run for 10 min gave about 10% unreacted SnH_4, H_2 ($>$ 90%), CO, unmeasured $Fe(CO)_5$ and $Fe_3(CO)_{12}$ (**1a**) (16%), a combined fraction 2 + 3 (not measured, and with major decomposition) and **3** (14%). In further 20 min runs, yields of **1** and **3** were similarly in the 15–20% range, but enhanced recovery of the mixed fraction was achieved by chromatography on silica plates, eluting with 1/1 CH_2Cl_2/hexane and stopping runs at the point where the orange and brown bands had just separated from the rest, removing from the silica, and completing work-up by fractional recrystallisation.

In reactions at 20 °C, or at 35 °C, metallic films of tin appeared within 24 h (6 h at 35 °C) and only H_2 (85–100%), CO, and $Fe(CO)_5$ were found in the volatile fraction while $Fe_3(CO)_{12}$ was the only species soluble in CH_2Cl_2. At 70 °C, formation of $Fe_3(CO)_{12}$ dominated even very short-period reactions.

Characterisation of 1. Electron probe analysis showed Sn/Fe = 1/3.3. A mass spectrum gave a parent ion centred at $m/e = 789$ with the Sn isotope pattern, together with 16 CO loss fragments and $SnFe_x^+$ for $x = 3, 2, 1$. In dichloromethane solution, the infrared spectrum showed CO stretches at (cm^{-1}): 2072 s, 2044 vs, 2027 m, and 2010 s, in agreement with literature values [1], while the solution showed Raman shifts at (cm^{-1}); 2106 m, p; 2075 vw, 2054 vw, 2029 vs, 2010 ms, 1980 w (only strong polarisations detectable). In a CsI disc, infrared absorptions were (cm^{-1}): 2106 w, 2072 m, 2054 w, sh, 2044 vs, 2026m, 2018 w, 2009 s, 1983 s, 1964 sh. Raman shifts from the solid were (cm^{-1}): 2105 m, 2076 vw, 2051 vw, 2033 w, 2020 vs, 2009 w sh, 2006 m, 1972 w.

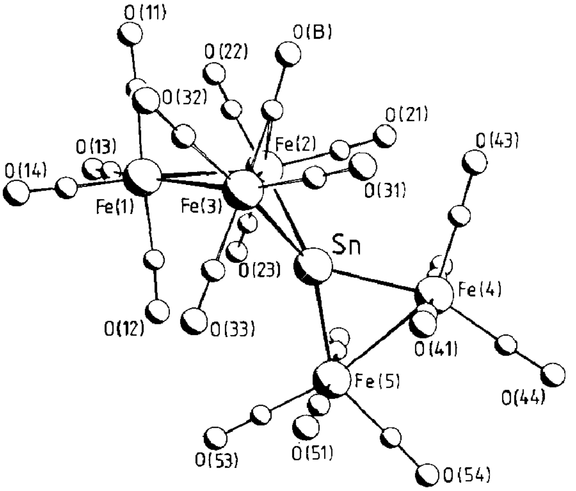

Fig. 1. A view of a molecule of $SnFe_5(CO)_{19}$ (**3**).

Table 2

Final positional and equivalent thermal parameters for $SnFe_5(CO)_{19}$

Atom	x	y	z	U_{eq}
Sn(1)	0.3395(1)	0.4109(1)	0.2801(1)	0.036
Fe(1)	−0.0014(1)	0.6802(1)	0.1554(1)	0.045
Fe(2)	0.3168(1)	0.5823(1)	0.1463(1)	0.038
Fe(3)	0.1404(1)	0.6507(1)	0.2897(1)	0.040
Fe(4)	0.5807(1)	0.2907(1)	0.3561(1)	0.042
Fe(5)	0.3647(1)	0.1686(1)	0.3318(1)	0.045
C(11)	0.005(1)	0.8509(9)	0.1228(5)	0.057
O(11)	−0.0010(7)	0.9577(6)	0.1012(4)	0.074
C(12)	0.0056(9)	0.5106(9)	0.1940(5)	0.052
O(12)	0.0019(7)	0.4054(6)	0.2143(4)	0.067
C(13)	−0.015(1)	0.6623(8)	0.0515(5)	0.057
O(13)	−0.0187(8)	0.6481(7)	−0.0144(4)	0.090
C(14)	−0.210(1)	0.7471(8)	0.1953(5)	0.060
O(14)	−0.3372(7)	0.7903(6)	0.2206(5)	0.089
C(21)	0.526(1)	0.5464(8)	0.1372(4)	0.050
O(21)	0.6569(7)	0.5297(6)	0.1282(3)	0.070
C(22)	0.303(1)	0.6893(8)	0.0494(5)	0.054
O(22)	0.3043(7)	0.7512(6)	−0.0157(3)	0.075
C(23)	0.3197(9)	0.4424(8)	0.1024(4)	0.050
O(23)	0.3243(8)	0.3581(6)	0.0689(3)	0.070
C(31)	0.238(1)	0.6670(8)	0.3666(5)	0.057
O(31)	0.2921(9)	0.6859(7)	0.4182(4)	0.097
C(32)	−0.011(1)	0.8102(8)	0.2988(4)	0.052
O(32)	−0.1047(7)	0.9113(5)	0.3104(4)	0.076
C(33)	0.0261(9)	0.5558(8)	0.3567(5)	0.050
O(33)	−0.0505(7)	0.5037(6)	0.4040(4)	0.076
C(41)	0.4517(9)	0.3475(8)	0.4492(5)	0.058
O(41)	0.3747(8)	0.3863(7)	0.5081(4)	0.082
C(42)	0.7003(9)	0.2390(8)	0.2598(5)	0.056
O(42)	0.7827(8)	0.2092(7)	0.1999(4)	0.081
C(43)	0.638(1)	0.434(1)	0.3382(5)	0.057
O(43)	0.6741(9)	0.5274(7)	0.3251(4)	0.086
C(44)	0.713(1)	0.1588(8)	0.4183(5)	0.062
O(44)	0.7994(8)	0.0800(7)	0.4586(4)	0.097
C(51)	0.238(1)	0.2227(8)	0.4266(5)	0.054
O(51)	0.1517(8)	0.2479(6)	0.4856(4)	0.084
C(52)	0.476(1)	0.1326(7)	0.2306(5)	0.057
O(52)	0.5448(9)	0.1036(6)	0.1676(4)	0.089
C(53)	0.210(1)	0.1311(9)	0.3051(6)	0.074
O(53)	0.107(1)	0.1058(8)	0.2898(6)	0.116
C(54)	0.483(1)	0.0148(9)	0.3841(5)	0.062
O(54)	0.5563(8)	−0.0853(6)	0.4169(4)	0.092
C(1B)	0.2736(9)	0.7370(8)	0.2051(4)	0.049
O(1B)	0.3117(7)	0.8322(6)	0.1965(4)	0.069
Cl(1S)	0.316(2)	0.049(2)	0.008(1)	0.087
Cl(2S)	0.320(2)	0.063(2)	1.033(1)	0.099
Cl(3S)	0.378(2)	0.096(1)	0.985(1)	0.122
C(1S)	0.507(4)	0.063(3)	0.972(2)	0.129

From fractions 2 + 3, extraction and crystallisation yielded mixtures with different compositions, allowing bands to be approximately assigned assuming there are only two components as (cm^{-1}): (a) 2088 ms, 2064 w sh, 2053 vs, 2037 vs, 2015 w, 2002 w sh, (b) 2090 m, 2054 vs, 2037 s, 2017 ms. These compare with those of the germanium analogues $Ge_2Fe_6(CO)_{23}$ and $Ge_2Fe_7(CO)_{26}$, respectively [9].

The least mobile band gave green crystals of **3**, soluble in dichloromethane but only sparingly soluble in hexane. Electron probe analysis showed 1 Sn/4.9 Fe. The mass spectrum showed the parent ion at 930 ± 3 for ^{119}Sn (calc. 931) together with 19 fragment ions attributed to CO loss (with the usual reservation that loss of Fe may overlap with loss of 2CO) and $SnFe_x$ for $x = 5, 4, 3, 2, 1$.

The IR spectrum, run in a 3/1 pentane/CH_2Cl_2 mixture was quite simple, with bands at (cm^{-1}) 2080s, 2052s, 2037 vs, 2002 m,br, and 1823 vw. In a CsI disc more bands were apparent and the bridging frequency shifted markedly; 2107 w, 2082 s, 2053 s, 2031 sh s, 2016 vs, 2002 s, 1980 mw, 1954 w, 1797 ms. The values and intensities of the terminal frequencies in solution are close to those reported [15] for the very similar $HBiRu_5(CO)_{18}$.

Xray structure of $SnFe_5(CO)_{19}$ (3)

Dark-green thin plates were obtained on slow cooling of a concentrated solution of $SnFe_5(CO)_{19}$ in CH_2Cl_2. Preliminary precession photography showed no symmetry higher than triclinic. Cell dimensions and intensity data were obtained using a Nicolet XRD P3 diffractometer using monochromated Mo-K_α X-rays. A view of the molecule is shown in Fig. 1.

Crystal data. $C_{19}Fe_5SnO_{19} \cdot 0.5CH_2Cl_2$, $M = 972.59$, triclinic, space group $P\bar{1}$, a 9.179(2), b 10.825(3), c 16.565(4) Å, α 78.67(2), β 78.22(2), γ 68.75(2)°, U

Table 3

Selected bond lengths and angles for $SnFe_5(CO)_{19}$.

Bond lengths (Å)			
Sn(1)–Fe(2)	2.587(1)	Fe(1)–Fe(2)	2.705(1)
Sn(1)–Fe(3)	2.590(1)	Fe(1)–Fe(3)	2.711(2)
Sn(1)–Fe(4)	2.566(1)	Fe(2)–Fe(3)	2.658(1)
Sn(1)–Fe(5)	2.535(1)	Fe(4)–Fe(5)	2.878(2)
Fe(2)–C(B)	1.984(8)	Fe(3)–C(B)	1.995(8)
Bond angles (°)			
Fe(2)–Sn(1)–Fe(3)	61.8(1)	Sn(1)–Fe(2)–Fe(1)	99.1(1)
Fe(2)–Sn(1)–Fe(4)	128.2(1)	Sn(1)–Fe(2)–Fe(3)	59.2(1)
Fe(2)–Sn(1)–Fe(5)	141.7(1)	Fe(1)–Fe(2)–Fe(3)	60.7(1)
Fe(3)–Sn(1)–Fe(4)	127.8(1)	Sn(1)–Fe(3)–Fe(1)	98.9(1)
Fe(3)–Sn(1)–Fe(5)	140.9(1)	Sn(1)–Fe(3)–Fe(2)	59.0(1)
Fe(4)–Sn(1)–Fe(5)	68.7(1)	Fe(1)–Fe(3)–Fe(2)	60.5(1)
Fe(2)–Fe(1)–Fe(3)	58.8(1)	Sn(1)–Fe(4)–Fe(5)	55.1(1)
Sn(1)–Fe(5)–Fe(4)	56.2(1)	Fe(2)–C(B)–Fe(3)	83.8(8)
Dihedral angles (°)			
Fe(1)Fe(2)Fe(3)/SnFe(2)Fe(3)	123.1		
Fe(1)Fe(2)Fe(3)/Fe(2)Fe(3)C(B)	105.7		
SnFe(2)Fe(3)/Fe(2)Fe(3)C(B)	131.2		
SnFe(2)Fe(3)/SnFe(4)Fe(5)	90.0		

1488.2(7) Å^3. D_c 2.17 g cm^{-3} for $Z = 2$. $F(000)$ 934, μ(Mo-K_α) 34 cm^{-1}, T 23°C, crystal size 0.40 × 0.36 × 0.03 mm. Intensity data in the range $0 < 2\theta < 55°$ were collected using Wycoff scans. Absorption corrections were applied based on a series of ϕ-scans, transmission factors 0.51 (min) to 0.93 (max). A total of 6195 unique reflections were measured and those 3922 with $I > 3\sigma(I)$ were used in all calculations.

The positions of the heavy atoms were found by direct methods (SHELXS86 [19]) and the full structure was routinely developed. A penultimate difference map showed some residual electron density corresponding to ca. 0.5 molecules of CH_2Cl_2, and this was included in the refinement with each Cl disordered over three sites. In the final cycles of full-matrix least-squares refinement all atoms of the complex were assigned anisotropic temperature factors. Refinement converged with $R = 0.0449$, $R_w = 0.0415$, with $w = [\sigma^2(F) + 0.000213F^2]^{-1}$, with no final shifts greater than 0.1σ, and with no residual electron density > 0.6 e Å^{-3}. Calculations were performed with SHELX76 [19]. The final positional parameters are given in Table 2, with selected bond parameters in Table 3.

Acknowledgements

We thank the New Zealand Universities Grants Committee and the donors of the Petroleum Research Fund, administered by the ACS, for financial support, and Dr Ward T Robinson, University of Canterbury, for collection of X-ray intensity data.

References

1 J.D. Cotton, S.A.R. Knox, I. Paul, and F.G.A. Stone, J. Chem. Soc. A, (1967) 264.
2 P.F. Lindley and P. Woodward, J. Chem. Soc. A, (1968) 382.
3 A.S. Batsanov, L.V. Rybin, M.I. Rybinskaya, Yu.T. Struchkov, I.M. Salimgareeva, and N.B. Bogatova, J. Organomet. Chem., 249 (1983) 319.
4 D. Melzer and E. Weiss, J. Organomet. Chem., 255 (1983) 335.
5 K.H. Whitmire, C.B. Lagrone, M.S. Churchill, J.C. Fettinger, and B.H. Robinson, Inorg. Chem., 26 (1987) 3491.
6 S.G. Anema, G.C. Barris, K.M. Mackay, and B.K. Nicholson, J. Organomet. Chem.. 350 (1988) 207.
7 R.F. Gerlach, K.M. Mackay, B.K. Nicholson and W.T. Robinson, J. Chem. Soc., Dalton Trans., (1981) 80.
8 K.M. Mackay, B.K. Nicholson, A.W. Sims and C.C. Tan, Acta Cryst. C, 43 (1987) 633.
9 S.G. Anema, K.M. Mackay, and B.K. Nicholson, Inorg. Chem., Paper IC890058D-0-4-0.
10 H.J. Emeléus and S.F.A. Kettle, J. Chem. Soc., (1958) 2444.
11 F.A. Cotton and J.M. Troup, J. Am. Chem. Soc., 96 (1974) 4155.
12 M.I. Bruce, B.K. Nicholson, and A.H. White, J. Organomet. Chem., 240 (1982) C33.
13 L.F. Dahl and J.F. Blount, Inorg. Chem., 4 (1965) 1373.
14 I. Brudgam, H. Hartl and D. Lentz, Z. Naturforsch. B, 39 (1984) 721.
15 B.F.G. Johnson, J. Lewis, P.R. Raithby and A.J. Whitton, J. Chem. Soc., Chem. Commun., (1988) 401.
16 S.A.R. Knox and F.G.A. Stone, J. Chem. Soc. A, (1971) 2874; A. Brookes, S.A.R. Knox and F.G.A. Stone, ibid., (1971) 3469.
17 C.J. Cardin, D.J. Cardin, G.A. Lawless, J.M. Power, M.B. Power, M.B. Hursthouse, J. Organomet. Chem., 325 (1987) 203.
18 K.M. Mackay and B.K. Nicholson, in G. Wilkinson, F.G.A. Stone, and E. Abel (Eds.), Comprehensive Organometallic Chemistry, Pergamon Press, 1982, Chp. 42.
19 G.M. Sheldrick, SHELXS86, a Program for Solving Crystal Structures, University of Gottingen, 1986: SHELX76, a Program for Crystal Structure Determination, University of Cambridge, 1976.